Self-Assembly via Adsorbate-Driven Dislocation Reactions

K. Thürmer,[1] C. B. Carter,[2] N. C. Bartelt,[1] and R. Q. Hwang[1,*]

[1]*Sandia National Laboratories, Livermore, California 94550, USA*

[2]*Department of Chemical Engineering and Materials Science, University of Minnesota, Minneapolis, Minnesota 55455, USA*

(Received 8 September 2003; published 9 March 2004)

Deposition of S onto a monolayer of Ag/Ru(0001) transforms the herringbone pattern of the clean Ag film into a strikingly regular array of 2D-vacancy islands [K. Pohl *et al.*, Nature (London) **397**, 238 (1999)]. Time-resolved scanning tunneling microscopy reveals that this nanometer-scale restructuring occurs by a cooperative mechanism involving the sequential formation of triangular regions with fcc and hcp stacking. Using a 2D Frenkel-Kontorova model, we can simulate the creation of these triangular building blocks via basic dislocation motions and reactions.

DOI: 10.1103/PhysRevLett.92.106101 PACS numbers: 68.35.Fx, 61.72.Lk, 68.37.Ef, 68.55.–a

Structures with nanometer-scale periodicities are often observed in thin-film heteroepitaxy. These patterns typically occur to accommodate the misfit between the lattice constants of the film and substrate. For these patterns to form, large numbers of atoms must move in a coordinated way. How this motion occurs is for the most part unknown. The purpose of this Letter is to determine the mechanisms of the rearrangement in detail for one particularly well-characterized system—the S-induced restructuring of Ag films on Ru [1,2]. Despite the relative simplicity of the initial and final states of the films, we find that the restructuring occurs by an intriguing sequence of dislocation creations and reactions.

When a monolayer of Ag on Ru is exposed to S, it transforms from one ordered nanometer-scale structure, depicted in Fig. 1(a), into a very different well-ordered pattern, shown in Fig. 1(b). In the initial state, the Ag-atom density is 92.86% of the Ru-substrate density; the linear defects between the ''elbows'' of the herringbone reconstruction visible in Fig. 1(a) are Shockley partial dislocations in which the Ag-Ag atomic spacing is the same as Ru along the line but expanded in the perpendicular direction. The final state consists of an arrangement of vacancy islands (or ''holes'') filled with S. The density of Ag between the holes has decreased to 90.2% of the Ru density, with the Ag-Ag lattice spacings being approximately isotropic.

As we describe below, this seemingly complex process of surface restructuring can be broken down into basic steps, which individually lower the energy by increasing the area fraction covered by S and by reducing the density of Ag atoms in the film. The crucial step is the formation of 5 nm wide triangular patches of either hcp or fcc stacking bounded by partial dislocations and S holes at the corners, which we refer to as ''stacking triangles.'' These triangles result from a dislocation reaction, which can be reproduced in a 2D Frenkel-Kontorova model based on first-principles parameters. Finally, the highly ordered nanostructure of Fig. 1(b) is completed by connecting these triangles through a sequence of dislocation climb [3] and annihilation.

The initial film was obtained in an ultrahigh vacuum system by depositing slightly more than a monolayer (ML) Ag onto the clean Ru(0001) surface followed by a flash to 520 °C. During S deposition from an electrochemical cell [4] we monitored the S_{64} peak in a mass spectrometer calibrated with scanning tunneling microscopy (STM) images of atomically resolved S on 0.9 ML Ag/Ru(0001) films to determine the S coverage.

Bulk Ag has a 7% larger nearest-neighbor distance than Ru. Studying the equilibrium structure of 1 ML Ag on Ru(0001) Hwang *et al.* [5] observed a herringbone pattern [6,7] with a 6 nm × 4 nm unit cell for a Ag coverage below and a 20 nm × 4 nm unit cell above saturation of the first monolayer. We studied extensively both coverage regimes but highly ordered S-hole arrays could be prepared only on films with a Ag coverage slightly more than 1 ML. The material in excess of 1 ML forms a partial second ML, which serves as a reservoir for Ag displaced by S.

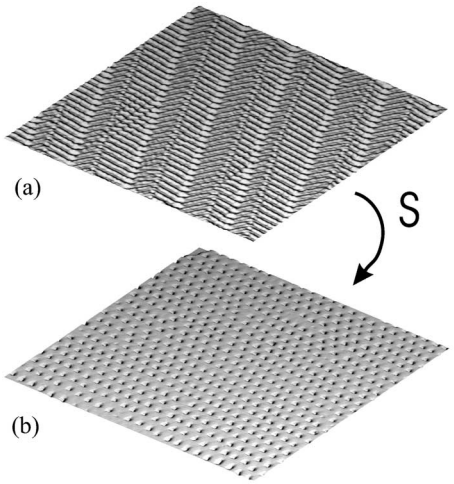

FIG. 1. 125 nm × 125 nm STM images showing initial and final states of adsorbate-induced surface reordering. (a) The equilibrium structure of 1 ML Ag/Ru(0001), displaying a herringbone pattern, transforms upon exposure to S into (b) a very stable triangular array of S-filled holes.

Figure 2(a) depicts the initial surface for our experiments, 1 ML of Ag on Ru(0001). S was deposited while continuously scanning the surface with the STM tip. The time sequence of STM images shown in Figs. 2(b)–2(d) illustrates the emergence of holes in the Ag film filled with S. The displaced Ag attaches to the second Ag-layer step, which we observed to advance (not shown). Similarly to the growth of Ni islands on Au(111) [6], S holes appear first at the elbows of the herringbone structure [Fig. 2(b)]. Upon subsequent S deposition, clusters of holes develop and grow [Figs. 2(d) and 4(a)] until, eventually; the entire surface is covered by a regular hole lattice [Figs. 1(b) and 4(f)].

To help understand why S displaces Ag atoms we used the first-principles local-density-approximation (LDA) VASP package [8,9] to estimate the energy gain for a S atom to displace a Ag atom on Ru. The difference in energy between a S atom adsorbed in a dilute 3×3 overlayer on Ru and a S atom on a pseudomorphic Ag film is 2.0 eV. On the other hand, the energy of Ag atoms in a pseudomorphic first layer is only 0.3 eV lower than Ag atoms in bulk Ag (approximating the second layer reservoir of Ag atoms). Thus S binds so strongly to the Ru substrate that it is favorable for the S to push Ag into the second layer. To understand the observed sequence of film patterns, we consider its dislocation structure [6,10]. Figure 2(e) shows a schematic of the herringbone reconstruction. To accommodate the 7% lattice mismatch, every 14th Ag-atom row is missing creating dislocations between the film and the substrate. These dislocations are split up into Shockley partials separating regions of fcc and hcp stacking. Film atoms above these misfit dislocations populate bridge sites and appear darker in STM [5]. A difference in apparent height of ≈ 0.03 Å allows the fcc and hcp regions to be distinguished though the assignment to the respective stacking types is uncertain. At points where Shockley partials with different Burgers vectors meet, threading dislocations are located [labeled as a red T in Fig. 2(e)]. These defects represent end points of surplus atom rows and are characterized by a perfect Burgers vector. Parallel to the partial dislocation lines the film adopts the smaller lattice spacing of the substrate thus retaining some excess atom density. This surplus Ag-atom density and the very strong binding of S to the substrate provide the context in which the steps of the film transformation can be explained.

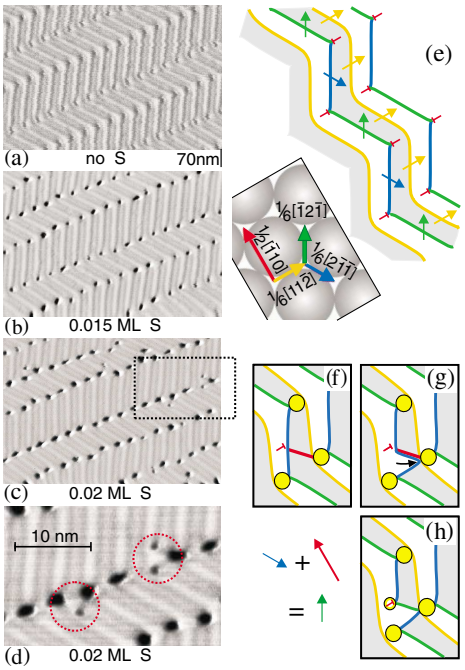

FIG. 2 (color). (a)–(c) Time sequence of STM images acquired during S deposition at room temperature, showing the early stages of surface restructuring. Misfit dislocations, separating regions of fcc and hcp stacking, appear as dark lines. (d) Zoom into the area marked by a rectangle in (c). (e) Dislocation structure in the herringbone pattern. A color code distinguishes different Burgers vectors. The shadings of fcc and hcp regions match the apparent height of the respective areas in the STM images. (f)–(h) Formation of a stacking triangle broken down into (f) extraction of a row of Ag atoms, (g) dislocation glide, and (h) dislocation reaction.

The STM image in Fig. 2(b) shows that the herringbone is first attacked at its elbows where the lattice is most distorted and film atoms occupy the energetically least favorable sites. Figures 2(b)–2(d) and 4(a) reveal that as the holes become larger, their center shifts to the convex side of the bend. Since here the clean film has the highest atom density, local extraction of Ag eliminates the areas of highest compressive stress. Figures 2(c) and 2(d) show the emergence of new smaller holes about 5 nm apart from existing ones. These new holes are located only on those partial dislocations that are bounded by threading dislocations. The stacking region on the convex side of the threading dislocation invades the area between the new hole and the nearest two old holes creating a triangular extension [bright triangles in Fig. 2(d)].

We propose a mechanism, based on simple dislocation motions and reactions, which leads to the formation of these stacking triangles. For the sake of clarity we present the involved events as a sequence of steps ignoring any overlap in time. First, Ag atoms are extracted along a line, drawn red in Fig. 2(f). From each close-packed atom row in the $[\underline{1}10]$ direction that is crossed by the red line, one atom is removed. Upon film closure this line becomes a perfect dislocation with an edge component terminated in threading dislocations. (A similar adsorbate-induced "cut" into the surface had been reported for oxygen on Cu/Ru [9].) Insertion of a small S hole at the end of this cut nearly eliminates the distortion energy of the threading dislocations. Then, a section of the partial dislocation, drawn in blue in Fig. 2(g), glides and aligns with the (red) perfect dislocation. Finally both dislocations react and produce a partial dislocation [Fig. 2(h), green line], with the Burgers vector given by the sum of the original vectors ($\frac{1}{6}[2\underline{1}1] + \frac{1}{2}[\underline{1}10] \rightarrow \frac{1}{6}[\underline{1}2\underline{1}]$). This reaction renders the new hole-decorated threading

dislocation equivalent to an elbow. Forming these stacking triangles accomplishes two goals. First, more Ru area is covered by S and, second, the compressive film stress is further relieved by the reductions in Ag-atom density.

Since the creation of these stacking triangles constitutes the key process of the film transformation, it warrants validation in an atomic model. We focus on the rearrangements that occur after extraction of the Ag atoms. These rearrangements are naturally modeled in a 2D Frenkel-Kontorova (FK) model [11], where nearest-neighbor film atoms are connected by elastic springs and are allowed to relax in the film plane. The substrate is represented by a fixed sinusoidal potential. The corresponding surface energy is given by

$$E = \sum_i V_S(r_i) + \sum_j V_F(l_j),$$

with the first sum representing the sinusoidal substrate potential as a function of the 2D film atom positions r_j. The second sum includes all nearest-neighbor bonds within the film. For most simulations we used a harmonic in-film potential $V_F(l) = k/2 \times (l - b \times a_{\mathrm{Ru}})^2$, where l is the bond length, k is the "spring" constant of the bond, and b is the preferred Ag-Ag distance measured in units of the Ru lattice spacing a_{Ru}. For our standard parameter set [12] we used values based on LDA calculations reported by Thayer *et al.* [13].

Figure 3(a) shows the unit cell used in the simulations. The brightness of the circles reflects the substrate potential at the respective site. The red or green color between the circles indicates the type of stacking (fcc vs hcp). The starting configuration has been generated from a pseudomorphic layer by extracting rows of atoms along the $\sqrt{3}$ directions $[\underline{1}2\underline{1}]$ and $[2\underline{1}1]$. Upon relaxation, each missing row evolves into two Shockley partials (bright lines)

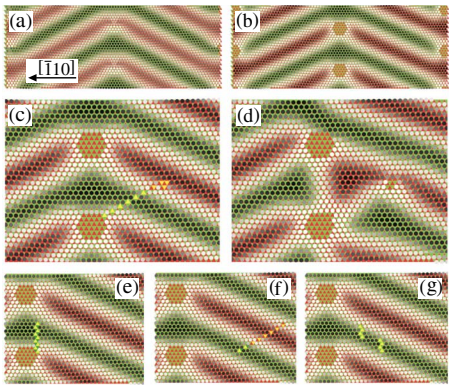

FIG. 3 (color). FK simulation of (a) the clean Ag/Ru(0001) film, (b) relaxed surface after decorating the elbows, (c) zoom into the configuration obtained from (b) by removing film atoms to create a line of vacancies and a small hole. This initial state relaxes via a dislocation reaction into the configuration (d) forming a stacking triangle. Panels (e)–(g) show examples of configurations of extracted atoms that also relax to (d).

yielding the herringbone pattern. The S-filled holes at the elbows are mimicked in the FK model by removing atoms inside circles centered at the threading dislocations. After relaxation the system assumes the configuration depicted in Fig. 3(b) resembling closely the experimentally observed patterns. To verify our explanation of the stacking triangle formation, we need to reproduce the three-step process of Figs. 2(f)–2(h). To initiate this process we extracted film atoms along a line as described above and shown in Fig. 2(f). Upon film closure this line constitutes a perfect dislocation with a Burgers vector $\frac{1}{2}[\underline{1}10]$. Though it was not a prerequisite for the process to occur, we removed two atoms at the end of this line to mimic the new small S hole. Figure 3(c) illustrates this starting configuration. Then, after the model system is allowed to relax, it evolves into the surface structure depicted in Fig. 3(d). The striking similarity to stacking triangles observed with STM [see Figs. 2(c), 2(d), and 4(a)], corroborates our notion about their nature. The pattern of extracted atoms shown in Fig. 3(c) was chosen to be closest to the final lowest-energy state of the surface. However, the system can readily find the low energy state even if the atoms are extracted in much different locations. For example, the configurations shown in Figs. 3(e)–3(g) all relax to Fig. 3(d). This occurs because the dislocations created by the extraction process can glide towards the holes. Thus the self-assembly process we observe is not dependent on which Ag atoms are most "reactive" to S. The role of S-filled holes is geometrical: the process we observe does not depend on the structure of S within the holes, for example. Our conclusions are also independent of the details of the FK model: we varied the parameters E_{top}, E_{brdg}, and the spring constant k from $\frac{1}{3}$ to 3 times the value of the standard set and the stacking-fault energy E_{hcp} from 0 to 40 meV/atom (= 101 mJ/m^2). In addition, we replaced the harmonic intralayer potential by a Morse potential $V_F(l) = V_0 \times \{1 - \exp[-2\alpha(l - ba_{\mathrm{Ru}})/(ba_{\mathrm{Ru}})]\}^2 - V_0$: Every parameter set for which the initial herringbone structure was stable leads to the formation of the stacking triangle.

These triangles served as building blocks during the subsequent restructuring. The STM image of Fig. 4(a), taken at a later stage than Figs. 2(c) and 2(d), shows an increased number of stacking triangles, most of which are incorporated in S-hole clusters. Figure 4(b) illustrates that after a row of triangles has formed the dislocation reactions can easily be repeated. In contrast to the reported case of S on Cu/Ru [14], where S binds strongly to the threading dislocations and promotes their proliferation, the less reactive Ag is simply pushed away. This facilitates the process depicted in Fig. 4(c), which lowers the energy by eliminating threading dislocations. Through extraction of surplus Ag atoms from their compressed convex side, threading dislocations climb [3] and annihilate, leaving behind a dislocation node connecting adjacent stacking triangles. This process, in conjunction

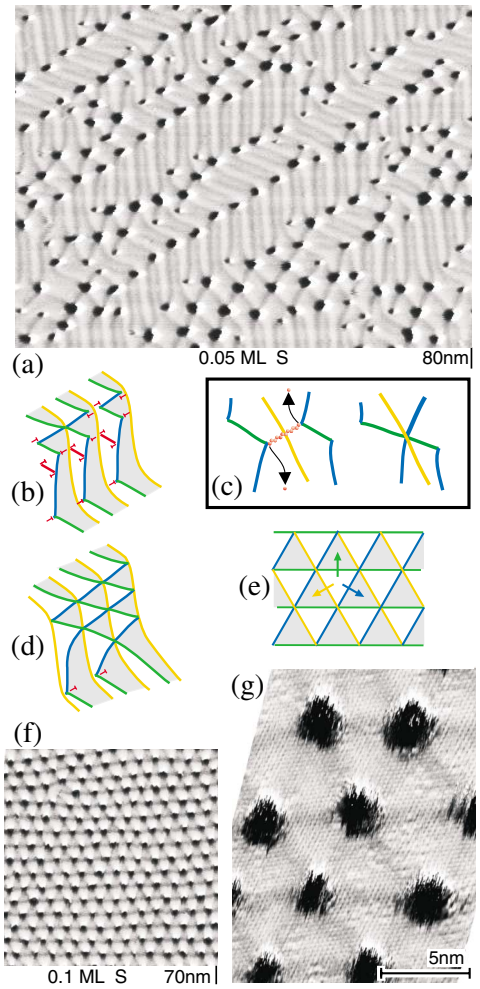

FIG. 4 (color). (a) STM image showing the emergence of local hole arrays. (b) The configuration after formation of a row of stacking triangles. (c) Adjacent threading dislocations climb and annihilate. The resulting nodes of partial dislocations are decorated by S holes (not shown). (d) Dislocation structure of a local S-hole array and (e) a completed hole array. (f),(g) STM images of the complete S-hole array. (f) Triangles of fcc and hcp stacking appear in a different brightness. (g) Small-scale image resolving Ag atoms and Shockley partials connecting the S holes.

with the creation of new stacking triangles, leads to local S-hole arrays [Figs. 4(a) and 4(d)], which eventually merge into a complete hole lattice [Fig. 4(e)].

STM images of the fully restructured film [Figs. 4(f) and 4(g)] exhibit a surface with threefold symmetry. The sulfur holes are arranged in a remarkably ordered triangular lattice. Partial dislocations connecting the holes can be discerned as slightly darker bands. At the dislocation nodes Ag would have to occupy on-top sites. This energetically unfavorable configuration is avoided by keeping the nodes decorated with S holes. The stability of hole lattice and dislocation network are mutually dependent. The elimination of on-top sites by decorating the dislocation nodes makes this structure energetically stable. On the other hand, the S holes are kept apart and thus prevented from merging, because they are tied to the evenly spaced dislocation nodes.

The assembly of ordered patterns in thin films often involves changes in density. For the S-induced restructuring of Ag films on Ru reported in this Letter, we infer that these density changes occur by the creation of edge dislocations. These dislocations interact with existing dislocations as well as point defects through a well-defined sequence of reactions to create the final ordered state independent of the details of how individual atoms are extracted from the film. Since edge dislocation creation is a general method of changing density, we expect that the cooperative events necessary for self-assembly to occur on the nanometer length scale will often involve dislocation creation and motion. The fact that we can reproduce much of the observed motion with a simple 2D Frenkel-Kontorova model is thus encouraging progress in our ability to predict the mechanisms of self-assembly.

We are grateful to Karsten Pohl and Roland Stumpf for helpful discussions. This research was supported by the Office of Basic Energy Sciences, Division of Material Sciences, U.S. Department of Energy, under Contract No. DE-AC04-94AL85000.

*Present address: Brookhaven National Laboratories, Upton, NY 11973.

[1] K. Pohl, M. C. Bartelt, J. de la Figuera, N. C. Bartelt, J. Hrbek, and R. Q. Hwang, Nature (London) **397**, 238 (1999).
[2] K. Pohl *et al.*, Surf. Sci. **433–435**, 506 (1999).
[3] J. P. Hirth and J. Lothe, *Theory of Dislocations* (Krieger, Malabar, FL, 1992).
[4] G.-Q. Xu and J. Hrbek, Catal. Lett. **2**, 199 (1989).
[5] R. Q. Hwang, J. C. Hamilton, J. L. Stevens, and S. M. Foiles, Phys. Rev. Lett. **75**, 4242 (1995).
[6] D. D. Chambliss, R. J. Wilson, and S. Chiang, J. Vac. Sci. Technol. B **9**, 933 (1991); Phys. Rev. Lett. **66**, 1721 (1991).
[7] U. Harten, A. M. Lahee, J. P. Toennies, and C. Wöll, Phys. Rev. Lett. **54**, 2619 (1985).
[8] G. Kresse and J. Hafner, Phys. Rev. B **47**, 558 (1993); **49**, 14 251 (1994); G. Kresse and J. Furthmüller, Comput. Mater. Sci. **6**, 15 (1996); Phys. Rev. B **54**, 11 169 (1996).
[9] J. de la Figuera, C. B. Carter, N. C. Bartelt, and R. Q. Hwang, Surf. Sci. **531**, 29 (2003).
[10] C. B. Carter and R. Q. Hwang, Phys. Rev. B **51**, 4730 (1995).
[11] F. C. Frank and J. H. van der Merwe, Proc. R. Soc. London **198**, 205 (1949).
[12] $k = 3800$ meV/Å^2, $b = 1.055$, substrate potential reproduces the LDA values for bridge-site energy $E_{\text{brdg}} = 55$ meV, on-top-site energy $E_{\text{top}} = 282$ meV, and $E_{\text{hcp}} = E_{\text{fcc}} = 0$.
[13] G. E. Thayer, N. C. Bartelt, V. Ozolins, A. K. Schmid, S. Chiang, and R. Q. Hwang, Phys. Rev. Lett. **89**, 036101 (2002).
[14] J. de la Figuera, K. Pohl, A. K. Schmid, N. C. Bartelt, J. Hrbek, and R. Q. Hwang, Surf. Sci. **433**, 93 (1999).